

# Adaptive Demodulation in Differentially Coherent Phase Systems: Design and Performance Analysis

J. David Brown<sup>†</sup>, Jamshid Abouei<sup>††</sup>, *Member, IEEE*, Konstantinos N. Plataniotis<sup>††</sup>, *Senior Member, IEEE* and Subbarayan Pasupathy<sup>††</sup>, *Life Fellow, IEEE*

<sup>†</sup> Ottawa, Canada, Tel: 613-236-1051, Email: david\_jw\_brown@yahoo.com

<sup>††</sup> The Edward S. Rogers Sr. Dept. of Electrical and Computer Engineering,

University of Toronto, Toronto, Canada, Emails: {abouei, kostas, pas}@comm.utoronto.ca

## Abstract

Adaptive Demodulation (ADM) is a newly proposed rate-adaptive system which operates without requiring Channel State Information (CSI) at the transmitter (unlike adaptive modulation) by using adaptive decision region boundaries at the receiver and encoding the data with a rateless code. This paper addresses the design and performance of an ADM scheme for two common differentially coherent schemes: M-DPSK (M-ary Differential Phase Shift Keying) and M-DAPSK (M-ary Differential Amplitude and Phase Shift Keying) operating over AWGN and Rayleigh fading channels. The optimal method for determining the most reliable bits for a given differential detection scheme is presented. In addition, simple (near-optimal) implementations are provided for recovering the most reliable bits from a received pair of differentially encoded symbols for systems using 16-DPSK and 16-DAPSK. The new receivers offer the advantages of a rate-adaptive system, without requiring CSI at the transmitter and a coherent phase reference at the receiver. Bit error analysis for the ADM system in both cases is presented along with numerical results of the spectral efficiency for the rate-adaptive systems operating over a Rayleigh fading channel.

- The first author completed his Ph.D. in ECE department at University of Toronto. This work was supported in part by a postgraduate scholarship from the Natural Sciences and Engineering Research Council of Canada (NSERC), an Industry Canada Fessenden postgraduate scholarship, and in part by an Ontario Research Fund (ORF) project entitled "Self-Powered Sensor Networks".

- The material in this paper was presented in part in the 18<sup>th</sup> Annual IEEE Int. Symposium on Personal, Indoor and Mobile Radio Communications (PIMRC'07), 2007 [1].

## Index Terms

Adaptive Demodulation (ADM), decision schemes, Differential Phase Shift Keying (DPSK), Differential Amplitude and Phase Shift Keying (DAPSK), rateless codes.

### I. INTRODUCTION

Rate-adaptive solutions such as adaptive modulation and incremental redundancy have proven to be very effective at increasing the spectral efficiency of wireless systems operating over a variety of channels [2]–[4]. These techniques allow mobile communications systems to operate efficiently over a wide range of channel parameters while maintaining a target Bit Error Rate (BER), as opposed to a non-rate-adaptive system which is designed for a worst-case “fixed-rate” channel. In a traditional implementation of adaptive modulation [5], the transmitter dynamically adjusts the current level of modulation based on feedback of the observed Channel State Information (CSI) from the receiver. The requirement of CSI at the transmitter is one of the major impediments of adaptive modulation systems, especially for a high-speed mobile receiver for which the channel information changes rapidly. Incremental redundancy [6] systems do not require CSI at the transmitter, but instead encode data packets using a low-rate “mother code” and break the message into smaller sub-packets, sending them one-by-one until the receiver acquires enough packets to successfully decode the message. These systems require the receiver to decode after each sub-packet is received to check for successful transmission and also require a buffer large enough (in poor channel conditions) to accommodate the entire collection of sub-packets, meaning that the complexity of the decoding operation varies with the quality of the channel.

Adaptive Demodulation (ADM), first proposed in [7] and with the expanded framework in [8], offers a new rate-adaptive solution that avoids the need for CSI at the transmitter (unlike adaptive modulation), has a fixed buffer size (roughly equal to the size of the message), and requires the receiver to perform a decoding operation only once (unlike incremental redundancy). In an ADM system, the transmitter sends data at a fixed-rate using a standard constellation and the receiver demodulates data at a non-fixed-rate using appropriately designed sets of decision regions chosen based on the CSI observed by the receiver. Before transmission, each  $k$ -bit message is encoded using a rateless erasure code (e.g. the Luby Transform

(LT) code [9] or the Raptor code [10]). To recover any  $k$ -bit message, the receiver simply buffers the demodulated (non-erased) bits until it has accumulated  $(1 + \varepsilon)k$  “reliable” bits (where  $\varepsilon$  is a small fixed quantity) at which point the original message can be decoded, regardless of the erasure pattern introduced in the message. In [7], the ADM-based receiver uses sets of specially designed decision regions to demodulate some or all of the bits in a transmitted symbol (depending upon the desired level of reliability), and assumes a “coherent phase reference” is available at the receiver. The optimal constellations and mappings for the ADM system over an additive white Gaussian noise (AWGN) channel and its performance for AWGN were derived in [7]. Particular instances of the ADM solution are the application studies considered in [11] and [12] for Gaussian relay channels.

In this paper, we consider how to implement the ADM system using differentially coherent detection: an attractive alternative when a reliable phase reference is not available. This is certainly a valid and interesting problem when the channel changes rapidly making phase coherence difficult or expensive to achieve. There are several works in the literature that study the performance analysis of differentially coherent detection in wireless RF applications (e.g., [13]) with focus on mobile satellite communications [14], and optical communication systems [15]. Of interest is to utilize the Differential Phase-Shift Keying (DPSK) in mobile communications systems which commonly circumvents the ambiguity in the phase recovery [16].

To the best of our knowledge, this is the first paper addressing this rate-adaptive technique with focus on differentially coherent detection in time-varying wireless systems. This paper studies the design and performance analysis of a hard-decision version of the ADM scheme for two common differentially coherent schemes: M-DPSK and M-DAPSK (M-ary Differential Amplitude and Phase Shift Keying) operating over AWGN and Rayleigh fading channels. The paper makes the following contributions:

- The optimal method for determining the most reliable bits for a given differential detection scheme is presented.
- Simple (near-optimal) implementations are provided for recovering the most reliable bits from a received pair of differentially encoded symbols for systems using 16-DPSK and 16-DAPSK. The

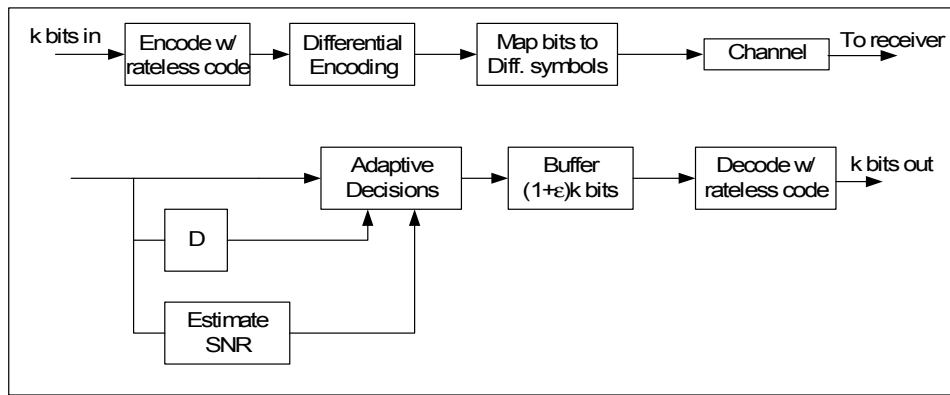


Fig. 1. Block diagram of a differential ADM transmitter/receiver.

new receivers offer the advantages of a rate-adaptive system, without requiring CSI at the transmitter and a coherent phase reference at the receivers.

- Bit error analysis for the ADM system in both cases is presented along with numerical results of the spectral efficiency for the rate-adaptive systems operating over a Rayleigh fading channel.

The rest of the paper is organized as follows. Section II provides an overview of the system under consideration and briefly introduces some ADM concepts and terminology. Section III presents the optimal method for determining the most reliable bits for a given differential detection scheme in the ADM-based system with 16-DPSK. With a similar argument as for the DPSK-ADM system model, Section IV deals with a simple (near-optimal) implementation for recovering the most reliable 1, 2, 3, or 4 bits from a received pair of differentially encoded symbols for systems using 16-DAPSK. Sections III and IV also include the Log-Likelihood Ratio (LLR) computation of each bit for every pair of received symbols. Section V includes the probability of error analysis for the near-optimal detection schemes and presents the spectral efficiency of ADM using differential detection. Finally, Section VI provides a brief summary and conclusions.

## II. SYSTEM MODEL AND ASSUMPTIONS

In this work, we consider an ADM-based single-hop wireless system depicted in Fig. 1, where the transmitter desires to send data packets of equal length toward the corresponding receiver using a predetermined rateless code and differential encoding. To send a  $k$ -bit data packet, the transmitter first encodes

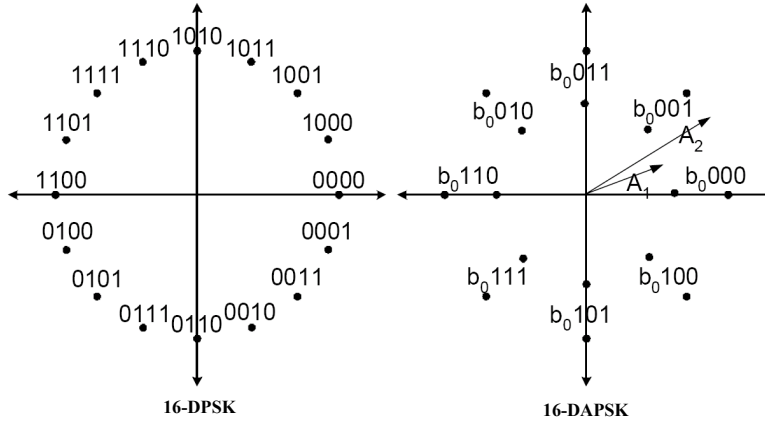


Fig. 2. Mappings of differential information for 16-DPSK and 16-DAPSK.

it using an LT (Luby Transform) code to produce a stream of coded bits. Such codes are a class of sparse-graph “rateless” erasure codes which are fully explained in [9] and [10]. It is shown in [17] that LT codes offer strong benefits in using in practical wireless networking applications with dynamic distance and position nodes. LT codes have a very simple encoding mechanism that allows the transmitter to produce a potentially limitless sequence of encoded bits from the original  $k$  message bits. Once the receiver successfully recovers any  $(1 + \varepsilon)k$  reliable encoded bits—where  $\varepsilon$  is determined by the reliability of the recovered bits—a message passing decoder using the *sum-product algorithm* [18], can be used to recover the original  $k$ -bit message.

The coded bits are used to produce differentially encoded symbols. In this paper, we consider two common differentially coherent schemes: 16-DPSK and 16-DAPSK. For 16-DPSK, the phase difference between successive symbols conveys 4 bits of information (here denoted by  $b_0b_1b_2b_3$ ) in the standard fashion of [19] with the mapping shown in Fig. 2, where  $b_i \in \{0, 1\}$ ,  $i = 0, 1, 2, 3$ . Differential Amplitude Phase Shift Keying is a popular alternative to DPSK and has a performance advantage over DPSK at the expense of slightly increased constellation complexity [20]. 16-DAPSK is implemented as described in [20] where the amplitude difference between successive symbols conveys 1 bit of information (here denoted by  $b_0$ ) and the phase difference conveys an additional 3 bits ( $b_1b_2b_3$ ), according to the mapping in Fig. 2. By convention, a change in amplitude (i.e., consecutive symbols are transmitted on different

rings) represents a “1” bit, while no change in amplitude represents a “0” bit. The differential symbols are transmitted over an AWGN channel<sup>1</sup>. For the remainder of the paper, we observe the following notation.

**DPSK:** After matched filtering, a sample of a 16-DPSK symbol at the receiver can be written as

$$y_k = s_k e^{j\theta_k} + n_k, \quad (1)$$

where  $s_k \triangleq e^{j\phi_k}$  represents a transmitted symbol with phase  $\phi_k$  and normalized symbol energy,  $\theta_k$  represents the arbitrary (and unknown) phase introduced by the channel, and  $n_k$  is a zero-mean circularly-symmetric complex Gaussian random variable with variance  $\sigma^2 = \frac{N_0}{2}$  in each dimension. It is assumed that  $\theta_k$  is constant over at least two symbol intervals such that  $\theta_k = \theta_{k-1}$ . In addition, we denote the phase difference between consecutive 16-DPSK symbols  $s_k$  and  $s_{k-1}$  by

$$\Delta\phi_k = \phi_k + \theta_k - (\phi_{k-1} + \theta_{k-1}) = \phi_k - \phi_{k-1}. \quad (2)$$

**DAPSK:** Similarly, adopting a notation akin to [20], we denote two consecutive received 16-DAPSK symbols (the  $(k-1)$ <sup>th</sup> and  $k$ <sup>th</sup> symbols) as follows:

$$z_{k-1} = d_{k-1} e^{j\theta_k} + n_{k-1}, \quad (3)$$

$$z_k = \alpha_k d_{k-1} e^{j\theta_k} + n_k, \quad (4)$$

where  $d_{k-1}$  is a complex quantity representing the magnitude and the phase of the  $(k-1)$ <sup>th</sup> symbol,  $\alpha_k$  is a complex quantity representing the change in magnitude and phase from the  $(k-1)$ <sup>th</sup> to the  $k$ <sup>th</sup> symbol, and  $n_k$  and  $n_{k-1}$  are independent Gaussian noise samples as above. We note that  $|d_{k-1}|$  can take on one of only two values:  $A_1 \triangleq \sqrt{\frac{2}{1+R^2}}$  or  $A_2 \triangleq R\sqrt{\frac{2}{1+R^2}}$ , where  $R \triangleq \frac{A_2}{A_1}$  is defined as the *ring ratio* in 16-DAPSK. The symbol energy is assumed to be normalized such that  $\frac{A_1^2 + A_2^2}{2} = 1$ . The change in magnitude,  $|\alpha_k|$ , can be one of three values:  $1/R$ ,  $1$ , or  $R$ . Clearly, only certain combinations of  $|d_{k-1}|$  and  $|\alpha_k|$  are allowable; for example, it would not be possible to have  $|d_{k-1}| = A_2$  and  $|\alpha_k| = R$ , since this would require the  $k$ <sup>th</sup> symbol to have magnitude not equal to either  $A_1$  or  $A_2$ . The following ordered

<sup>1</sup>The Rayleigh fading case will be considered later in Section V. For the fading channel model and as per the standard assumption in differential schemes, it is assumed that the complex channel gain is constant over at least two symbol intervals.

pairs  $(|d_{k-1}|, |\alpha_k|)$  specify the only allowable combinations of  $|d_{k-1}|$  and  $|\alpha_k|$ :  $(A_1, 1)$ ,  $(A_2, 1)$ ,  $(A_1, R)$ , and  $(A_2, 1/R)$ .

**Decision Scheme:** In the ADM system with differentially coherent detection, the receiver utilizes a  $\beta$ -Decision Scheme ( $\beta$ -DS) to recover the  $\beta$  most likely bits<sup>2</sup> transmitted based on the observation of two consecutive differentially encoded symbols as will be described in the subsequent sections. Indeed, the receiver uses the instantaneous Signal-to-Noise Ratio (SNR) to determine which  $\beta$ -DS to use to demodulate a pair of symbols in order to maintain a given BER,  $P_b$ , as a standard of reliability. For the above scheme, non-demodulated (unreliable) bits are erased. Demodulated (reliable) bits are buffered until the receiver has collected sufficient bits for decoding at which point the decoder returns the decoded  $k$ -bit message.

### III. OPTIMAL $\beta$ -DECISION SCHEMES FOR 16-DPSK

For a particular pair of differentially encoded symbols, the  $\beta$  most reliable bits in the output of the  $\beta$ -DS should be the  $\beta$  bits with the largest magnitude Log Likelihood Ratios (LLRs). Thus, the “optimal”  $\beta$ -DS is a device that computes the LLRs of each bit for every pair of received symbols, compares their magnitudes, and chooses the  $\beta$  bits with the largest LLRs. We begin with this construction and introduce several approximations that produce simple, near-optimal  $\beta$ -DSs with easy implementations that *do not* require any LLR computations.

Let  $B_{i,j}$  denote the set of all differential angles  $\Delta\phi$  such that bit  $b_i = j$ , where  $j \in \{0, 1\}$ . Thus, the likelihood ratio for  $b_i$  for two consecutive received symbols  $y_k$  and  $y_{k-1}$  can be written as

$$\Lambda_{b_i}(y_k, y_{k-1}) = \frac{\Pr(y_k, y_{k-1} | b_i = 0)}{\Pr(y_k, y_{k-1} | b_i = 1)} = \frac{\sum_{\Delta\phi_m \in B_{i,0}} \Pr(y_k, y_{k-1} | \Delta\phi_m)}{\sum_{\Delta\phi_\ell \in B_{i,1}} \Pr(y_k, y_{k-1} | \Delta\phi_\ell)}, \quad (5)$$

where  $\Pr(y_k, y_{k-1} | \Delta\phi_m)$  denotes the *a posteriori* probability of observing the pair of received symbols  $y_k$  and  $y_{k-1}$  given that differential angle  $\Delta\phi_m$  was encoded at the transmitter. Using a modified form of eqn. (9) in [21], it can be shown that

$$\Pr(y_k, y_{k-1} | \Delta\phi_m) = \frac{e^{-\frac{2+|y_k|^2+|y_{k-1}|^2}{2\sigma^2}}}{(2\pi\sigma^2)^2} I_0 \left( \frac{|y_k + y_{k-1} e^{j\Delta\phi_m}|}{\sigma^2} \right), \quad (6)$$

<sup>2</sup>For instance, for the 16-DPSK or 16-DAPSK,  $\beta \in \{1, 2, 3, 4\}$ .

where  $I_0(x)$  is the zeroth order modified Bessel function of the first kind. It is revealed from (6) that only the Bessel term of  $\Pr(y_k, y_{k-1} | \Delta\phi_m)$  is a function of  $\Delta\phi_m$ , thus allowing us to cancel the exponential leading terms that would appear in an expansion of (5). This results in  $\Lambda_{b_i}$  being the ratio of sums of Bessel terms, i.e.,

$$\Lambda_{b_i}(y_k, y_{k-1}) = \frac{\sum_{\Delta\phi_m \in B_{i,0}} I_0\left(\frac{|y_k + y_{k-1} e^{j\Delta\phi_m}|}{\sigma^2}\right)}{\sum_{\Delta\phi_\ell \in B_{i,1}} I_0\left(\frac{|y_k + y_{k-1} e^{j\Delta\phi_\ell}|}{\sigma^2}\right)}. \quad (7)$$

Note that  $I_0(x)$  is a rapidly increasing function of  $x$ , when  $x$  grows, and is approximated by  $I_0(x) \approx \frac{e^x}{\sqrt{2\pi x}}$ . Thus, for moderate to large values of SNR (i.e. when  $1/\sigma^2$  is large), the sums in (7) can both be well approximated by a single dominant term, since the argument of the Bessel function will be in the steep part of the curve. To find these dominant terms in (7), we observe that

$$|y_k + y_{k-1} e^{j\Delta\phi_m}| = \sqrt{|y_k|^2 + |y_{k-1}|^2 + 2|y_k||y_{k-1}|\cos(\phi_k - \Delta\phi_m)}, \quad (8)$$

where  $\phi_k$  denotes the phase difference between  $y_k$  and  $y_{k-1}$ . Clearly, (8) is maximized when the difference  $|\phi_k - \Delta\phi_m|$  is minimized; thus the dominant term in the sums of Bessel functions will be the term with encoded differential phase  $\Delta\phi_m \in B_{i,0}$  closest to the phase difference  $\phi_k$ . Let  $\Delta\phi_{i,0}$  denote the particular differential phase  $\Delta\phi_m \in B_{i,0}$  such that  $|\phi_k - \Delta\phi_m|$  is minimized. Similarly, let  $\Delta\phi_{i,1}$  denote the particular differential phase  $\Delta\phi_\ell \in B_{i,1}$  such that  $|\phi_k - \Delta\phi_\ell|$  is minimized. With these definitions and under the high SNR approximation, (7) can be written as

$$\Lambda_{b_i}(y_k, y_{k-1}) \approx \frac{I_0\left(\frac{1}{\sigma^2} \sqrt{|y_k|^2 + |y_{k-1}|^2 + 2|y_k||y_{k-1}|\cos(\phi_k - \Delta\phi_{i,0})}\right)}{I_0\left(\frac{1}{\sigma^2} \sqrt{|y_k|^2 + |y_{k-1}|^2 + 2|y_k||y_{k-1}|\cos(\phi_k - \Delta\phi_{i,1})}\right)}. \quad (9)$$

To find the  $\beta$ -DSs, the values of  $|\ln(\Lambda_{b_i}(y_k, y_{k-1}))|$  must be compared for all  $b_i$  over the range  $0 < \phi_k \leq 2\pi$ . To simplify this comparison, we define  $\Delta\phi_{i,min}$  to be the value of  $\Delta\phi_{i,0}$  or  $\Delta\phi_{i,1}$  for which  $|\phi_k - \Delta\phi_{i,min}|$  is minimized and  $\Delta\phi_{i,max}$  to be the value of  $\Delta\phi_{i,0}$  or  $\Delta\phi_{i,1}$  for which  $|\phi_k - \Delta\phi_{i,max}|$  is maximized. For example, if  $0 < \phi_k < \pi/16$  then  $\Delta\phi_{2,min} = \Delta\phi_{2,0} = 0$  and  $\Delta\phi_{2,max} = \Delta\phi_{2,1} = -\pi/4$ . Some thought reveals that *all*  $\Delta\phi_{i,min}$  will be equal for all  $b_i$  for any given value of  $\phi_k$  (i.e.,  $\Delta\phi_{0,min} = \Delta\phi_{1,min} = \Delta\phi_{2,min} = \Delta\phi_{3,min}$ ). However, this is not true in general for  $\Delta\phi_{i,max}$ <sup>3</sup>.

<sup>3</sup>Continuing the example of  $0 < \phi_k < \pi/16$ , we will have  $\Delta\phi_{i,min} = 0$  for all  $i$ , and  $\Delta\phi_{0,max} = \pi/8$ ,  $\Delta\phi_{1,max} = -\pi/2$ ,  $\Delta\phi_{2,max} = -\pi/4$  (as above), and  $\Delta\phi_{3,max} = -\pi/8$ .

Since

$$\begin{aligned} I_0 \left( \frac{1}{\sigma^2} \sqrt{|y_k|^2 + |y_{k-1}|^2 + 2|y_k||y_{k-1}| \cos(\phi_k - \Delta\phi_{i,min})} \right) &> \\ I_0 \left( \frac{1}{\sigma^2} \sqrt{|y_k|^2 + |y_{k-1}|^2 + 2|y_k||y_{k-1}| \cos(\phi_k - \Delta\phi_{i,max})} \right) &, \end{aligned} \quad (10)$$

then we can write

$$\begin{aligned} |\ln(\Lambda_{b_i}(y_k, y_{k-1}))| &\approx \ln \left( I_0 \left( \frac{1}{\sigma^2} \sqrt{|y_k|^2 + |y_{k-1}|^2 + 2|y_k||y_{k-1}| \cos(\phi_k - \Delta\phi_{i,min})} \right) \right) - \\ &\ln \left( I_0 \left( \frac{1}{\sigma^2} \sqrt{|y_k|^2 + |y_{k-1}|^2 + 2|y_k||y_{k-1}| \cos(\phi_k - \Delta\phi_{i,max})} \right) \right). \end{aligned} \quad (11)$$

Noting the fact that all  $\Delta\phi_{i,min}$  are equal for all  $i$ , comparing the values of  $|\ln(\Lambda_{b_i}(y_k, y_{k-1}))|$  can be achieved by comparing  $\ln \left( I_0 \left( \frac{1}{\sigma^2} \sqrt{|y_k|^2 + |y_{k-1}|^2 + 2|y_k||y_{k-1}| \cos(\phi_k - \Delta\phi_{i,max})} \right) \right)$  for all  $i$ . Finally, using the fact that  $\ln(x)$  and  $I_0(x)$  are both monotonic increasing, it can be shown that this comparison reduces to the following simple decision rules:

$$|\phi_k - \Delta\phi_{i,max}| > |\phi_k - \Delta\phi_{j,max}| \rightarrow |\ln(\Lambda_{b_i}(y_k, y_{k-1}))| > |\ln(\Lambda_{b_j}(y_k, y_{k-1}))|, \quad (12)$$

$$|\phi_k - \Delta\phi_{i,max}| < |\phi_k - \Delta\phi_{j,max}| \rightarrow |\ln(\Lambda_{b_i}(y_k, y_{k-1}))| < |\ln(\Lambda_{b_j}(y_k, y_{k-1}))|. \quad (13)$$

Using the decision rules in (12) and (13), it is a simple matter to determine the  $\beta$ -DSs to recover the most likely 1, 2, and 3 bits for each pair of 16-DPSK symbols. The receiver simply computes the phase difference  $\phi_k$  between consecutive symbols and uses this angle to demodulate  $\beta$  bits based on the regions given in Fig. 3, where the regions are derived from the decision rules above.

#### IV. OPTIMAL $\beta$ -DECISION SCHEMES FOR 16-DAPSK

Recalling the notation from (3) and (4), the standard method used to demodulate 16-DAPSK is to compute the decision statistics  $r_k \triangleq \frac{|z_k|}{|z_{k-1}|}$  and  $\psi_k \triangleq \arg(z_k) - \arg(z_{k-1})$ . Typically, the  $r_k$  statistic is used to make a decision on the amplitude bit ( $b_0$ ), while the  $\psi_k$  statistic is used to decide on the phase bits ( $b_1 b_2 b_3$ ). We determine the optimal  $\beta$ -DSs of 16-DAPSK to find the most likely 1, 2, or 3 bits based on the observed  $r_k$  and  $\psi_k$ .

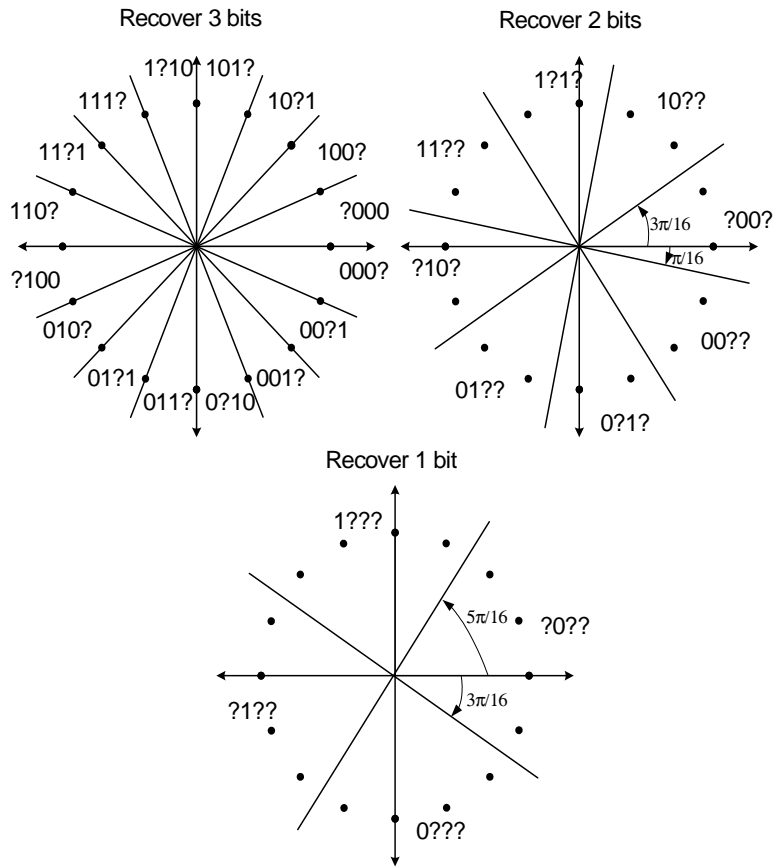


Fig. 3.  $\beta$ -decision scheme for 16-DPSK to recover 1, 2, and 3 bits for a pair of differential symbols.

Proceeding in a similar fashion to Section III, define  $C_{i,j}$  to be the set of all triples  $(|d_{k-1}|, |\alpha_k|, \arg(\alpha_k))$  such that bit  $b_i = j$ , where  $j \in \{0, 1\}$ . The likelihood ratio for  $b_i$  for the received statistics  $r_k$  and  $\psi_k$  is thus given by

$$\begin{aligned} \Lambda_{b_i}(r_k, \psi_k) &= \frac{\Pr(r_k, \psi_k | b_i = 0)}{\Pr(r_k, \psi_k | b_i = 1)} \\ &= \frac{\sum_{(|d_{k-1}|, |\alpha_k|, \arg(\alpha_k))_m \in C_{i,0}} \Pr(r_k, \psi_k | (|d_{k-1}|, |\alpha_k|, \arg(\alpha_k))_m)}{\sum_{(|d_{k-1}|, |\alpha_k|, \arg(\alpha_k))_\ell \in C_{i,1}} \Pr(r_k, \psi_k | (|d_{k-1}|, |\alpha_k|, \arg(\alpha_k))_\ell)}. \end{aligned} \quad (14)$$

Using eqn. (3.21) to (3.30) in [22], it can be shown that

$$\Pr(r_k, \psi_k | (|d_{k-1}|, |\alpha_k|, \arg(\alpha_k))) = \frac{e^{\frac{\xi^2}{B} - P}}{(\sigma^2)^2 \pi B^3} (\xi^2 + B) r_k, \quad (15)$$

where

$$\xi^2 \triangleq \left( \frac{|d_{k-1}|}{\sigma^2} \right)^2 (1 + |\alpha_k|^2 r_k^2 + 2|\alpha_k| r_k \cos(\psi_k - \arg(\alpha_k))), \quad (16)$$

$$P \triangleq \frac{|d_{k-1}|^2}{\sigma^2} (1 + |\alpha_k|^2), \quad \text{and} \quad (17)$$

$$B \triangleq \frac{1 + r_k^2}{\sigma^2}. \quad (18)$$

A useful property of (14) when the *a posteriori* probabilities are given as in (15) is that  $\Lambda_{b_i}(r_k, \psi_k)$  has the same value for  $r_k$  as for  $\frac{1}{r_k}$ . Thus, any  $\beta$ -DS for 16-DAPSK can compute  $r'_k \triangleq \min(r_k, \frac{1}{r_k}) \leq 1$  and use this value for detection without loss of accuracy. This simplifies the decision schemes since the analysis can be confined to values of  $r'_k$  contained within the unit circle. Intuitively, it makes sense that  $r_k$  and  $\frac{1}{r_k}$  would lead to the same reliability since it should not matter the order we transition from one ring to the other (since either way we will have one point on the large ring and one on the small ring).

Note that  $e^x$  is a rapidly increasing function of  $x$ , when  $x$  grows. Thus, for moderate to large values of SNR and with a similar argument as for 16-DPSK, it turns out that the sums in the numerator and denominator of (14) can be approximated by a single dominant term. Further simplifications arise by noting that the denominator of (15) and the multiplicative  $r_k$  term are common to all terms in (14) and thus will cancel. Additionally, at high SNR we note that  $\xi^2 \gg B$ , so we drop the additive  $B$  term from (15). Thus, the numerator and denominator of the likelihood ratio in (14) can be approximated by appropriately chosen dominant terms of the form  $\xi^2 e^{\frac{\xi^2}{B} - P}$ . With some thought, it is possible to identify the values of  $|d_{k-1}|$ ,  $|\alpha_k|$ , and  $\arg(\alpha_k)$  that maximize (15) for any particular pair of  $(r_k, \psi_k)$ .

#### A. Simple Estimate for Choosing the Differential Amplitude Threshold

Before determining the  $\beta$ -DSs for 16-DAPSK, we develop an interesting result obtained from the high SNR estimate of (14). In standard 16-DAPSK systems, the decision for the “differential amplitude bit”  $b_0$  is to choose  $b_0 = 0$  when  $r'_k > \Delta_0$  and to choose  $b_0 = 1$  when  $r'_k < \Delta_0$ , where  $\Delta_0$  is an appropriately chosen threshold based on the ring ratio  $R$ . An optimal value of  $\Delta_0$  can be found by numerically evaluating (14) for  $i = 0$  where  $\Delta_0$  is the value of  $r'_k$  such that  $\Lambda_{b_0}(r'_k, \psi_k) = 1$ , i.e.,  $b_0 = 0$  and  $b_0 = 1$  are equally likely. The high SNR estimate of (14) can be used to develop a remarkably simple (and accurate) estimate

for the threshold  $\Delta_0$ . At high SNR (and for the range  $1/R < r'_k < 1$ ), the dominant terms in (14) are  $\Pr(r_k, \psi_k | (A_1, 1, \phi))$  in the numerator and  $\Pr(r_k, \psi_k | (A_2, 1/R, \phi))$  in the denominator, with  $\phi$  representing the differential angle closest to  $\psi_k$ . A final approximation can be made by observing that  $\phi$  will always be within  $\pm\pi/8$  of differential angle  $\psi_k$ ; using this fact, we use  $\cos(\psi_k - \phi) \approx 1$ . Thus, at high SNR we can write

$$\Lambda_{b_0}(r_k, \psi_k) \approx e^Z \frac{\left(\frac{A_1}{\sigma^2}\right)^2 (1 + r_k^2 + 2r_k)}{\left(\frac{A_2}{\sigma^2}\right)^2 (1 + r_k^2/R^2 + 2r_k/R)} \quad (19)$$

$$\stackrel{(a)}{=} \frac{e^Z}{R^2} \left( \frac{1 + r_k}{1 + \frac{r_k}{R}} \right)^2, \quad (20)$$

where (a) comes from  $R \triangleq \frac{A_2}{A_1}$ , and

$$Z \triangleq \frac{1}{\sigma^2(1 + r_k^2)} \left( A_2^2 \left( \frac{1}{R} - r_k \right)^2 - A_1^2 (1 - r_k)^2 \right). \quad (21)$$

To find  $\Delta_0$ , we want to find the  $r_k$  such that the estimate in (19) is equal to 1. At high SNR, the behavior of the exponential determines, to a large extent, whether  $\Lambda_{b_0}(r_k, \psi_k)$  is greater than or less than 1. That is, to a reasonable approximation,  $e^Z \gg 1$  when  $r_k > \Delta_0$  and  $e^Z \ll 1$  when  $r_k < \Delta_0$  (at high SNR); due to the dominant behavior of the exponential,  $\text{sign}(Z)$  gives a reasonable estimate of whether or not  $\Lambda_{b_0}(r_k, \psi_k)$  exceeds 1. Consequently, a simple estimate for  $\Delta_0$  is found by solving for  $r_k$  when  $Z = 0$ . Solving (21) when  $Z = 0$ , results in

$$\Delta_0 \approx r_k|_{Z=0} = \frac{2}{1 + R}. \quad (22)$$

This approximation has been verified to be accurate to within two percent of the optimum value obtained through numerical solution [8] (over the useful range  $1.5 < R < 2.5$ ). For  $R = 2$ , results in [23] (and numerical evaluation of (14)) report an optimal value of  $\Delta_0 = 0.68$  while the estimate gives  $\Delta_0 \approx 2/3 = 0.667$ .

### B. Optimal $\beta$ -Decision Scheme

To compute the  $\beta$ -DSs for 16-DAPSK, we first identify the dominant terms in the numerator and denominator of (14). Then, we use these estimates to compare the likelihood ratios of each bit in a

similar fashion to the way  $\Delta_0$  was determined above. Adopting a notation similar to what was used in Section III, let  $\Delta\psi_{i,0}$  denote the particular phase  $\arg(\alpha_k)$  (where  $(|d_{k-1}|, |\alpha_k|, \arg(\alpha_k)) \in C_{i,0}$ ) such that  $|\psi_k - \Delta\psi_{i,0}|$  is minimized, and define  $\Delta\psi_{i,1}$  in the same manner. Furthermore, denote by  $\Delta\psi_{i,min}$  the value of  $\Delta\psi_{i,0}$  or  $\Delta\psi_{i,1}$  for which  $|\psi_k - \Delta\psi_{i,min}|$  is minimized, and denote by  $\Delta\psi_{i,max}$  the value of  $\Delta\psi_{i,0}$  or  $\Delta\psi_{i,1}$  for which  $|\psi_k - \Delta\psi_{i,max}|$  is maximized.

An example computation comparing likelihood ratios is given as follows. For  $\Delta_0 < r_k < 1$ , it can be shown that for  $i = 1, 2$ , or  $3$ , the numerator of (14) is dominated by  $\Pr(r_k, \psi_k | (A_1, 1, \Delta\psi_{i,0}))$  and the denominator is dominated by  $\Pr(r_k, \psi_k | (A_1, 1, \Delta\psi_{i,1}))$ . Additionally, it can be shown that for  $i = 0$ , the numerator is dominated by  $\Pr(r_k, \psi_k | (A_1, 1, \Delta\psi_{0,min}))$  and the denominator is dominated by  $\Pr(r_k, \psi_k | (A_2, 1/R, \Delta\psi_{0,min}))$ . Now since one of  $\Pr(r_k, \psi_k | (A_1, 1, \Delta\psi_{i,0}))$  and  $\Pr(r_k, \psi_k | (A_1, 1, \Delta\psi_{i,1}))$  *must be* equal to  $\Pr(r_k, \psi_k | (A_1, 1, \Delta\psi_{i,min}))$  (with the other equal to  $\Pr(r_k, \psi_k | (A_1, 1, \Delta\psi_{i,max}))$ ), then comparing  $|\ln(\Lambda_{b_0}(r_k, \psi_k))|$  with  $|\ln(\Lambda_{b_i}(r_k, \psi_k))|$  ( $i \neq 0$ ) amounts to evaluating the difference

$$\begin{aligned} & |\ln(\Lambda_{b_i}(r_k, \psi_k))| - |\ln(\Lambda_{b_0}(r_k, \psi_k))| \\ &= \ln(\Pr(r_k, \psi_k | (A_1, 1, \Delta\psi_{i,min}))) - \ln(\Pr(r_k, \psi_k | (A_1, 1, \Delta\psi_{i,max}))) \\ & \quad - (\ln(\Pr(r_k, \psi_k | (A_1, 1, \Delta\psi_{0,min}))) - \ln(\Pr(r_k, \psi_k | (A_2, 1/R, \Delta\psi_{0,min})))) \\ & \stackrel{(a)}{=} \ln(\Pr(r_k, \psi_k | (A_2, 1/R, \Delta\psi_{0,min}))) - \ln(\Pr(r_k, \psi_k | (A_1, 1, \Delta\psi_{i,max}))), \end{aligned} \quad (23)$$

where (a) comes from the fact that  $\Pr(r_k, \psi_k | (A_1, 1, \Delta\psi_{0,min})) = \Pr(r_k, \psi_k | (A_1, 1, \Delta\psi_{i,min}))$ , and noting that  $\Delta\psi_{i,min}$  are equal for all  $i \in \{0, 1, 2, 3\}$ . Finding the sign of the difference in (23) can be computed by evaluating the quotient

$$L \triangleq \frac{\Pr(r_k, \psi_k | (A_2, 1/R, \Delta\psi_{0,min}))}{\Pr(r_k, \psi_k | (A_1, 1, \Delta\psi_{i,max}))} \stackrel{(a)}{=} \frac{R^2 + r_k^2 + 2r_k R \cos(\psi_k - \psi_{0,min})}{1 + r_k^2 + 2r_k \cos(\psi_k - \psi_{i,max})} e^Z, \quad (24)$$

where  $Z \triangleq r_k(A_1/\sigma^2)^2(2R - 2\cos(\psi_k - \psi_{i,max}) - r_k(R^2 - 1))$ , and (a) follows from the estimate  $\cos(\psi_k - \psi_{i,min}) \approx 1$ . Using the same arguments made when evaluating the quotient in (19), at high SNR  $\text{sign}(Z)$  gives a reasonable estimate of whether or not  $L > 1$ . This results in the following decision rule (when  $\Delta_0 < r_k < 1$ ): if  $r_k < \frac{2}{R^2-1}(R - \cos(\psi_k - \psi_{i,max}))$  then  $b_i$  is more likely than  $b_0$ ; otherwise,  $b_0$  is more likely.

Using this technique to compare other likelihood ratios over other ranges of  $r_k$  we obtain the following simple set of decision rules to determine, for a given  $(r_k, \psi_k)$ , which bits are the most reliable:

- *Comparing*  $|\ln(\Lambda_{b_i}(r_k, \psi_k))|$  with  $|\ln(\Lambda_{b_j}(r_k, \psi_k))|$  for  $i, j \in \{1, 2, 3\}$ ,  $i \neq j$ :

$$|\psi_k - \Delta\psi_{i,max}| > |\psi_k - \Delta\psi_{j,max}| \rightarrow |\ln(\Lambda_{b_i}(r_k, \psi_k))| > |\ln(\Lambda_{b_j}(r_k, \psi_k))|. \quad (25)$$

- *Comparing*  $|\ln(\Lambda_{b_0}(r_k, \psi_k))|$  with  $|\ln(\Lambda_{b_i}(r_k, \psi_k))|$  for  $i \in \{1, 2, 3\}$ :

*i) When*  $r'_k > \Delta_0$ :

$$r'_k > \frac{2(R - \cos(\psi_k - \psi_{i,max}))}{R^2 - 1} \rightarrow |\ln(\Lambda_{b_0}(r_k, \psi_k))| > |\ln(\Lambda_{b_i}(r_k, \psi_k))|. \quad (26)$$

*ii) When*  $r'_k < \Delta_0$ :

$$r'_k > \frac{2(R \cos(\psi_k - \psi_{i,max}) - 1)}{R^2 - 1} \rightarrow |\ln(\Lambda_{b_i}(r_k, \psi_k))| > |\ln(\Lambda_{b_0}(r_k, \psi_k))|, \quad (27)$$

where  $\Delta_0$  is the decision threshold for  $b_0$ .

The decision rules in (25) to (27) are intuitively satisfying. When comparing only bits 1, 2, and 3 (i.e., the bits determined by the differential angle), rule (25) is identical to the decision rule for 16-DPSK (rule (12)), as one might expect. When  $\Delta_0 < r'_k < 1$ , rule (26) indicates that as  $(\psi_k - \psi_{i,max})$  increases<sup>4</sup> (i.e.,  $b_i$  becomes more reliable), then the right hand side of (26) will increase, meaning that  $r'_k$  must be large (i.e., close to 1) in order for  $b_0$  to be more reliable than  $b_i$ . Finally, when  $r'_k < \Delta_0$ , rule (27) indicates that as  $(\psi_k - \psi_{i,max})$  increases (i.e.,  $b_i$  becomes more reliable) then the right hand side of (27) decreases, meaning that  $r'_k$  must decrease ( $b_0$  becoming more reliable as  $r'_k$  gets further away from  $\Delta_0$ ) in order for  $b_0$  to be more reliable than  $b_i$ .

Despite the relative simplicity of the rules in (25) to (27) (compared to calculating and comparing LLRs), it turns out that when the rules are evaluated over all possible  $(r_k, \psi_k)$  they do not produce  $\beta$ -DSs that are particularly simple to implement, unlike 16-DPSK<sup>5</sup>. In the next subsection, we propose simple  $\beta$ -DSs for 16-DAPSK based on a heuristic analysis; subsequent judicious application of the rules in (25) to (27) allow us to lend some mathematical rigor to the simplified decision schemes.

<sup>4</sup>An increase in  $(\psi_k - \psi_{i,max})$  means that the nearest differential angle that will result in an error has become even further away from the observed differential angle. This indicates that the reliability of  $b_i$  has increased.

<sup>5</sup>The  $\beta$ -DSs so produced have non-linear boundaries specified by the polar form equations in (26) and (27)

### C. Simple $\beta$ -Decision Scheme for 16-DAPSK

Recalling from the definition of the threshold  $\Delta_0$ , we observe that when  $r'_k$  is close in value to  $\Delta_0$ , the bit  $b_0$  is very unreliable. In this case, our  $\beta$ -DS (for  $\beta < 4$ ) should always drop  $b_0$  as the most unreliable bit (we will specify below precisely how close  $r'_k$  needs to be to  $\Delta_0$  for this to apply). Thus for  $r'_k$  “close” to  $\Delta_0$ , decisions on  $b_1$ ,  $b_2$ , and  $b_3$  can be made using (25), resulting in a simple set of  $\beta$ -DSs (similar to the DPSK regions in Fig. 3). Conversely,  $b_0$  is at its most reliable when  $r'_k$  is “close” to 1 or  $r'_k$  is very small. So for these values of  $r'_k$ , the  $\beta$ -DS should always demodulate  $b_0$  and demodulate  $\beta-1$  bits of  $b_1$ ,  $b_2$ , and  $b_3$ , again using (25). Finally, we propose a “transition region” that applies for  $r'_k$  in some region between 1 (i.e.,  $b_0$  reliable) and  $\Delta_0$  (i.e.,  $b_0$  unreliable) and also for  $r'_k$  in a region between  $\Delta_0$  and 0 (i.e.,  $b_0$  very reliable once again). This transition region can be viewed as a hybrid of two regions: one region where  $b_0$  is always erased and another region where  $b_0$  is always kept. The decision scheme for the transition region is derived by careful consideration of the behavior of the optimum decision schemes that would be obtained by directly evaluating the likelihood ratios of (14) over all  $(r_k, \psi_k)$  (or directly implementing the rules in (25) to (27)). In actual fact, the optimum decision schemes transition gradually between the “ $b_0$  reliable” and “ $b_0$  unreliable” regions in a continuous manner, passing through our proposed “transition region” for certain particular value(s) of  $r'_k$ . Intuitively the proposed transition region is a satisfying “halfway” point between  $b_0$  reliable and  $b_0$  unreliable.

The simplified  $\beta$ -DSs are given in Fig. 4 for  $\beta \in \{1, 2, 3\}$ , where the “ $b_0$  reliable” region appears on the far left, the “transition region” appears in the middle, and the “ $b_0$  unreliable” region appears on the far right for each  $\beta$ -DS. Fig. 4 also introduces the threshold terms  $\Delta_{\beta,1}$ ,  $\Delta_{\beta,2}$ ,  $\Delta_{\beta,3}$ , and  $\Delta_{\beta,4}$  that are used by the decision schemes that recover  $\beta$  bits. For  $\Delta_{\beta,1} < r'_k \leq 1$  or  $r'_k < \Delta_{\beta,4}$ ,  $b_0$  is sufficiently reliable that it is always kept, while for  $\Delta_{\beta,3} < r'_k \leq \Delta_{\beta,2}$ ,  $b_0$  is sufficiently unreliable that it is always discarded. Also, for all other values of  $r'_k$ , the transition region is used. A method is presented below to find  $\Delta_{\beta,1}$ ,  $\Delta_{\beta,2}$ ,  $\Delta_{\beta,3}$ , and  $\Delta_{\beta,4}$  using (26) and (27).

Consider the 3-DS shown in Fig. 4. As  $r'_k$  begins decreasing (from 1), an optimal 3-DS would begin to transition from the “ $b_0$  reliable” region in a continuous fashion to the hybrid (middle) region. Fig. 5 shows

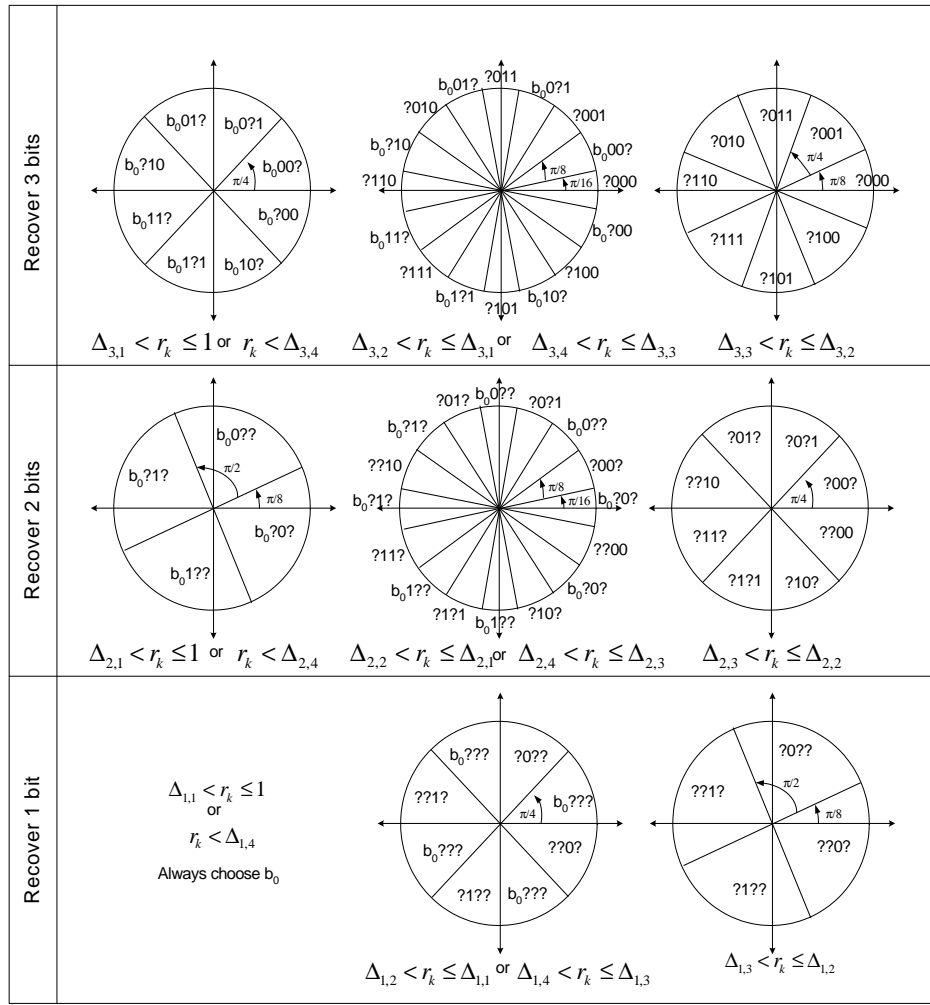
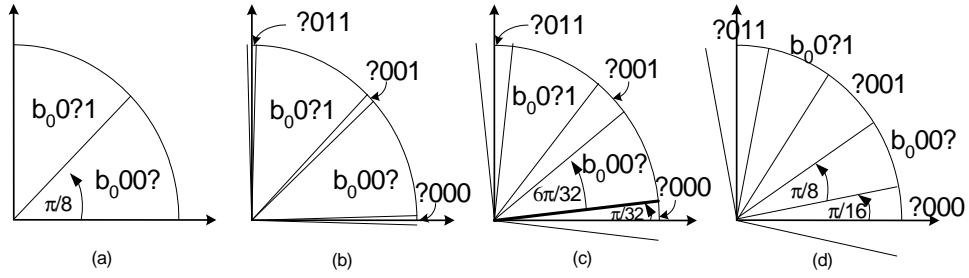
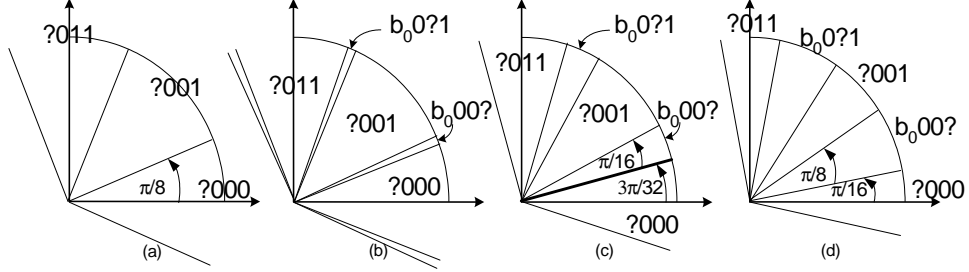


Fig. 4.  $\beta$ -Decision Scheme for 16-DAPSK to recover 1, 2, and 3 bits for a pair of differential symbols.

this progression; Fig. 5(a) shows a section of the  $b_0$  reliable region, while Fig. 5(b) shows the beginning of a transition to the hybrid region. In Fig. 5(b) we see that over the angles for which  $b_3$  is most reliable (as determined from rule (25)),  $b_0$  is dropped in favor of  $b_3$  when  $r'_k$  decreases by a sufficient amount. As  $r'_k$  continues to decrease, the angle over which  $b_3$  is selected (in favor of  $b_0$ ) grows as depicted in Fig. 5(c). Eventually this angle increases to such an extent that the decision region becomes the hybrid (middle) region shown in Fig. 5(d).

For the heuristic decision schemes depicted in Fig. 4 we opt use the “ $b_0$  reliable” region when the angle over which  $b_3$  is selected is small (as shown in Fig. 5(b)). We switch to the hybrid (middle) region when this angle has increased exactly halfway from zero to  $\pi/16$  (where  $\pi/16$  is the angle of the  $b_3$  region for the hybrid region as shown in Fig. 5(d)). This halfway point occurs as shown in Fig. 5(c), where


 Fig. 5. Progression from  $b_0$  reliable to “transition region”.

 Fig. 6. Progression from  $b_0$  unreliable to “transition region”.

the angle of the  $b_3$  region is  $\pi/32$ . The bold line in Fig. 5(c) depicts the boundary between choosing  $b_3$  and choosing  $b_0$ ; thus, the bold line represents the line such that  $\Lambda_{b_0}(r_k, \pi/32) = \Lambda_{b_3}(r_k, \pi/32)$ . To determine the  $r_k$  for which this equivalence occurs, we can use rule (26)<sup>6</sup> by direct substitution such that  $r'_k = \frac{2(R - \cos(\psi_k - \psi_{3,max}))}{R^2 - 1}$ , where  $\psi_k = \pi/32$  and  $\psi_{3,max} = \pi/4$  (the correct value for  $\psi_{3,max}$  can be determined from Fig.2(b)). This value of  $r_k$  is precisely the threshold  $\Delta_{3,1}$ .

As another example, to find the threshold  $\Delta_{3,2}$ , Fig. 6 proves useful as it depicts the transition from the “ $b_0$  unreliable” region to the hybrid region. Once again, Fig.6(c) shows the halfway point between these two regions such that the angle of the “ $b_0$  unreliable” region has decreased from  $4\pi/32$  to  $3\pi/32$ : exactly halfway to the angle  $2\pi/32$  shown in Fig.6(d). Using rule (26) we can find  $r'_k = \frac{2(R - \cos(\psi_k - \psi_{3,max}))}{R^2 - 1}$ , where  $\psi_k = 3\pi/32$  and  $\psi_{3,max} = \pi/4$ .

In a similar fashion, the remaining thresholds for all  $\Delta_{i,j}$  can be computed. Analytical equations for these thresholds computed in this manner are given in Table I. The equations for the thresholds are modified such that  $\Delta_{\beta,1}$  and  $\Delta_{\beta,2}$  can be no larger than 1 and  $\Delta_{\beta,3}$  and  $\Delta_{\beta,4}$  must be greater than 0. This

<sup>6</sup>Notice that we use (26) since here we are addressing the case where  $r'_k > \Delta_0$  as we have implicitly assumed that  $r'_k$  is large.

modification reflects the reality that  $0 \leq r'_k \leq 1$ . The table also evaluates the threshold equations for a ring ratio of  $R = 2$  which is the optimum ring ratio for standard 16-DAPSK in Rayleigh fading, as per [23]. Observe that some of the thresholds are equal to 1 or 0 indicating that some of the regions depicted in Fig. 4 are not used. Since Fig. 4 is general and applies for any  $R$ , not all regions will be used for every  $R$  since the thresholds themselves are functions of  $R$  by virtue of Table I.

TABLE I

EQUATIONS TO COMPUTE THRESHOLDS  $\Delta_{i,j}$  FOR 16-DAPSK.

$\Delta_{i,j}$	Equation	for $R = 2$
$\Delta_{3,1}$	$\min\left(1, \frac{2(R - \cos(\pi/32 - \pi/4))}{R^2 - 1}\right)$	0.818
$\Delta_{3,2}$	$\min\left(1, \frac{2(R - \cos(3\pi/32 - \pi/4))}{R^2 - 1}\right)$	0.745
$\Delta_{3,3}$	$\max\left(0, \frac{2(R \cos(3\pi/32 - \pi/4) - 1)}{R^2 - 1}\right)$	0.509
$\Delta_{3,4}$	$\max\left(0, \frac{2(R \cos(\pi/32 - \pi/4) - 1)}{R^2 - 1}\right)$	0.364
$\Delta_{2,1}$	$\min\left(1, \frac{2(R - \cos(3\pi/32 - (-\pi/4)))}{R^2 - 1}\right)$	1
$\Delta_{2,2}$	$\min\left(1, \frac{2(R - \cos(\pi/32 - (-\pi/4)))}{R^2 - 1}\right)$	0.910
$\Delta_{2,3}$	$\max\left(0, \frac{2(R \cos(\pi/32 - (-\pi/4)) - 1)}{R^2 - 1}\right)$	0.179
$\Delta_{2,4}$	$\max\left(0, \frac{2(R \cos(3\pi/32 - (-\pi/4)) - 1)}{R^2 - 1}\right)$	0
$\Delta_{1,1}$	$\min\left(1, \frac{2(R - \cos(3\pi/8 - (-\pi/4)))}{R^2 - 1}\right)$	1
$\Delta_{1,2}$	$\min\left(1, \frac{2(R - \cos(3\pi/16 - (-\pi/4)))}{R^2 - 1}\right)$	1
$\Delta_{1,3}$	$\max\left(0, \frac{2(R \cos(3\pi/16 - (-\pi/4)) - 1)}{R^2 - 1}\right)$	0
$\Delta_{1,4}$	$\max\left(0, \frac{2(R \cos(3\pi/8 - (-\pi/4)) - 1)}{R^2 - 1}\right)$	0

As a final note, we have verified that the simplified decision schemes of Fig. 4 perform nearly as well as the optimum (and complex) schemes obtained by numerically evaluating (14) or directly implementing the rules in (25) to (27). Numerical results demonstrating this fact are provided in Section V.

## V. PERFORMANCE OF DIFFERENTIALLY COHERENT ADM

To evaluate the performance of the ADM system for 16-DPSK and 16-DAPSK, we first examine the BER for each  $\beta$  decision scheme in AWGN. For 16-DAPSK, the BER can be computed by numerically integrating the density function in (15) over the appropriate regions of the simplified  $\beta$ -DSs as defined in Fig. 4. Additionally, we choose  $R = 2$  which is the optimum ring ratio for 16-DAPSK in Rayleigh

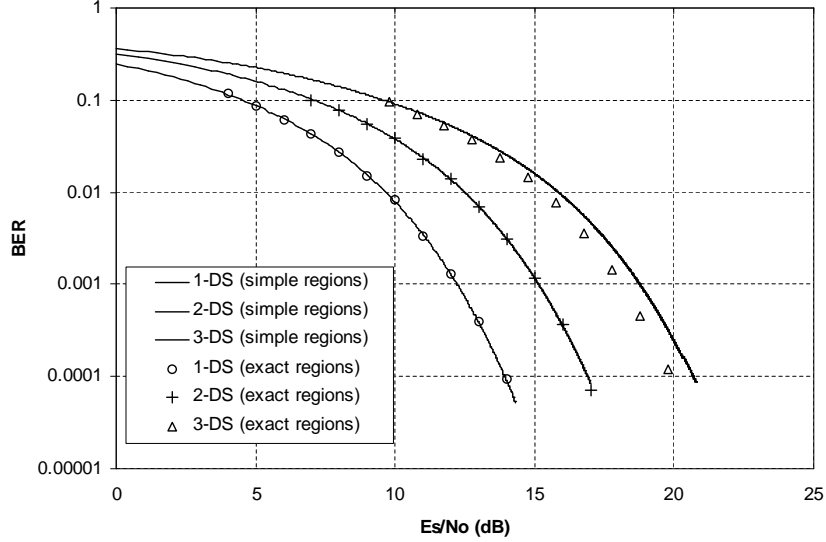


Fig. 7. Performance of the optimum decision schemes for 16-DAPSK and “simple” decision schemes.

fading [23]. The effect of the ring ratio in the proposed ADM system will be considered later. Fig. 7 illustrates the probability of error for the simplified  $\beta$  decision schemes for 16-DAPSK with  $R = 2$ . Also shown in Fig. 7 are BER curves (obtained through simulation) for the 16-DAPSK system using “optimal”  $\beta$  decision schemes that evaluate and compare the exact LLRs for every pair of received symbols. For  $\beta = 1$  and  $\beta = 2$  we observe virtually *no difference* in BER performance between the optimal and simplified  $\beta$ -DSs. For  $\beta = 3$ , the simplified scheme exhibits a loss of approximately 0.6dB at high SNR compared to the optimal scheme. Evaluating the BER at other values of  $R$  yield similar results (negligible loss for  $\beta = 1$  and  $\beta = 2$  and a small but measurable loss for  $\beta = 3$  at high SNR). These results suggest that the simplified  $\beta$ -DSs perform nearly as well as the optimum (and complex) schemes obtained by numerically evaluating (14).

For 16-DPSK, the probability of symbol error for a  $\beta$ -DS,  $P_{S,\beta}$ , can be computed as

$$P_{S,3} = 2 \int_{\pi/8}^{\pi} p(\phi) d\phi \tag{28}$$

$$P_{S,2} = \int_{3\pi/16}^{\pi} p(\phi) d\phi + \int_{-5\pi/16}^{-\pi} p(\phi) d\phi \tag{29}$$

$$P_{S,1} = \int_{5\pi/16}^{\pi} p(\phi) d\phi + \int_{-11\pi/16}^{-\pi} p(\phi) d\phi \tag{30}$$

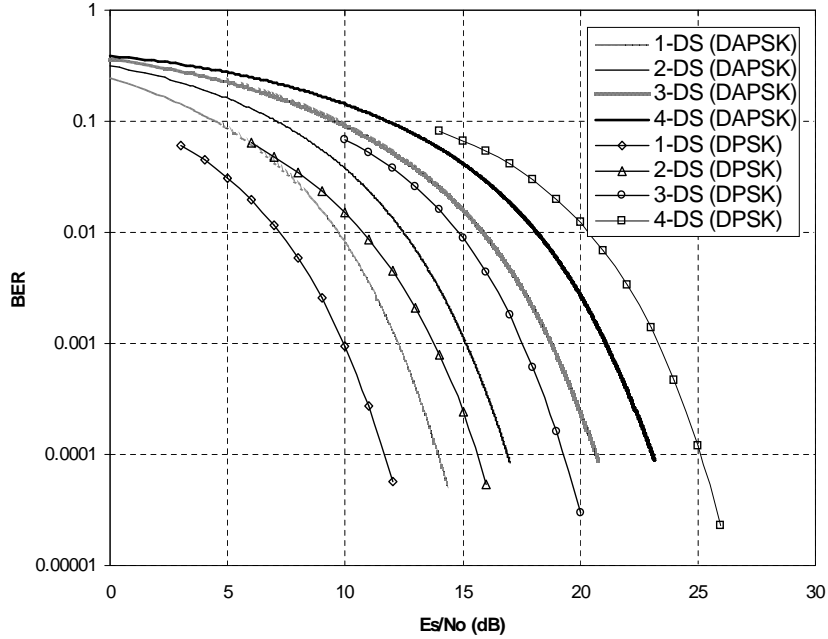


Fig. 8. BER for recovering 1, 2, 3, and 4 most likely bits for 16-DPSK and 16-DAPSK (with  $R = 2$ ).

where  $p(\phi)$  is the density of the phase angle between two vectors perturbed by (independent) AWGN samples. The integrals taken in the computation of the symbol error, above, are simply the integrals over the regions of received angle  $\Delta\phi_k$  for which an error would occur (based on the  $\beta$ -DSs given in Fig. 3). A good approximation for integrals of the form in (28) to (30) is given in [24], eqn. (46), rewritten in a slightly different form below:

$$\int_{\pi/M}^{\pi} p(\phi)d\phi \cong \frac{1}{2} \sqrt{\frac{1 + \cos(\pi/M)}{2 \cos(\pi/M)}} \operatorname{erfc} \sqrt{\gamma(1 - \cos(\pi/M))}, \quad M \geq 3, \quad (31)$$

where  $\operatorname{erfc}(x) \triangleq \frac{2}{\sqrt{\pi}} \int_x^{\infty} e^{-t^2} dt$  is the complementary error function.

Using (28) to (31), and making the approximation that the BER for a  $\beta$ -DS is  $\frac{1}{\beta} P_{S,\beta}$ , the probability of error curves for 16-DPSK are given in Fig. 8. The figure also provides the BER curves (from Fig. 7) for 16-DAPSK with  $R = 2$ . Note the initially surprising result that although 16-DAPSK outperforms 16-DPSK when recovering all four bits (as is well known), when recovering 1, 2, or 3 bits 16-DPSK shows a clear advantage over 16-DAPSK.

The fact that 16-DPSK outperforms 16-DAPSK for lower DS can be explained by noting that in a 16-DPSK scheme, certain bits are very well protected while others are more susceptible to error. By erasing

the error prone bits (for a given received angle) large gains are observed; however, for 16-DAPSK the bits are more uniformly reliable/unreliable with the consequence that erasing the least reliable among them will not result in gains as significant as for 16-DPSK. More specifically, for 16-DPSK, the least reliable bit (in general) is the bit that changes value between two differential angles denoting two “adjacent” symbols. When this bit is dropped (e.g., for 3-DS), the performance of the remaining bits is reminiscent of an 8-DPSK system—i.e., a significant gain is observed. With 16-DAPSK, an advantage is gained for 4-DS since the minimum differential angle separating differential symbols is  $\pi/4$  (as opposed to  $\pi/8$  for 16-DPSK). Of course, this increase in minimum angle is achieved by allowing for two distinct amplitudes:  $A_1$  and  $A_2$ . This strategy does indeed succeed in reducing the error rate of the least reliable bit. Often, however, the least reliable bit for a 16-DAPSK constellation is in fact the differential amplitude bit; thus, when this is neglected, the remaining bits are less reliable than for a 16-DPSK 3-DS since the inner ring necessarily has a smaller radius than the standard 16-DPSK radius (assuming equal symbol energies for the two constellations).

With the BER computed for all  $\beta$ -DSs, it is now possible to compute the optimal operating regions for the ADM system over a Rayleigh fading channel (i.e., compute which  $\beta$ -DS to use for a given observed instantaneous SNR). These operating regions are computed using the techniques outlined in [25] assuming that the fading is constant over at least two symbol intervals. Using the computed operating regions, the spectral efficiency (for “raw” uncoded bits) for ADM using 16-DPSK and 16-DAPSK is given in Fig. 9. It is seen that ADM using 16-DPSK outperforms ADM using 16-DAPSK for low rate transmission (until about 2.5 bits per symbol); additionally, it does not suffer a large performance deficit at higher rates. This is explained by the relatively poorer performance the 1-DS, 2-DS, and 3-DS of 16-DAPSK compared to 16-DPSK as noted in Fig. 8.

Although [23] demonstrated that a ring ratio of  $R \approx 2$  is an optimal choice for 16-DAPSK operating in a Rayleigh fading environment, it is not obvious that this ring ratio remains optimal for an ADM system using 16-DAPSK. Reference [8] demonstrates the effect of the ring ratio on the BER performance (in AWGN) for each  $\beta$  decision scheme. It is shown in [8] that for the 4-DS (i.e., standard 16-DAPSK

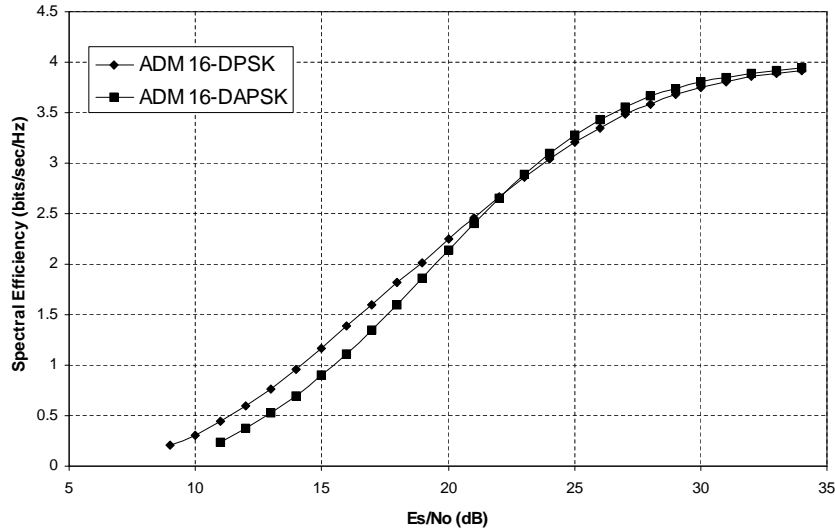


Fig. 9. Spectral Efficiency for 16-DPSK and 16-DAPSK (with  $R = 2$ ).

differentially coherent demodulation), the BER is minimized for a ring ratio of  $R = 2$ , a result that agrees with [23]. However, for the 3-DS, 2-DS, and 1-DS, it observed that the BER tends to increase with  $R$ , exhibiting no local minimum at  $R = 2$  (e.g., see Fig. 10 for 2-DS). Thus, for all  $\beta$ -DS except 4-DS, the BER performance improves for lower ring ratios. These results can be explained by observing that as  $R$  decreases below 2, the inner and outer ring radii become closer in value; consequently  $b_0$  becomes increasingly unreliable. This results in an increase in BER for 4-DS. For all other  $\beta$ -DS, however, the unreliable  $b_0$  is most likely the bit that will be discarded; the remaining bits become more reliable for smaller  $R$  since the radius of the inner ring increases, leading to more reliable angle measurements.

Since the BER of all  $\beta$ -DS (including 4-DS) increases when  $R > 2$ , we conclude that it is never advantageous (at least in terms of BER performance) to use ring ratios larger than 2 in the ADM system. The question still remains, however, what is the best ring ratio ( $R \leq 2$ ) for ADM. The answer depends on the desired system performance and range of operation. For example, if the system is expected to operate primarily in high average SNR at close to 4 bits per symbol, then  $R = 2$  is a good choice since the system will spend most of its time using 4-DS. However, if the system is expected to have a very broad range of operation, a smaller  $R$  may be advisable.

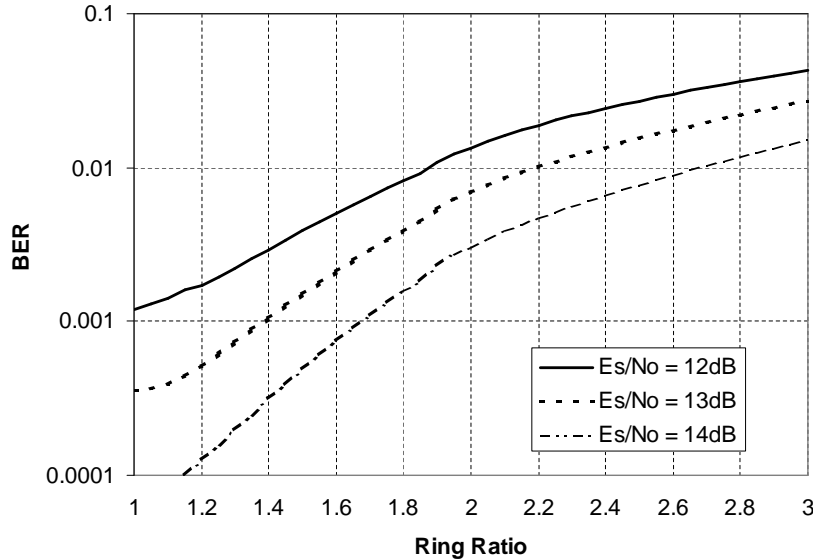


Fig. 10. BER of 16-DAPSK 2-DS for various ring ratios.

In Fig. 11, the spectral efficiency curves (for Rayleigh fading) are computed for a range of ring ratios. As expected, the ADM systems using low values of  $R$  outperform the ADM system using  $R = 2$  at lower rates; however, these systems are less effective at higher rates when the performance of the 4-DS becomes more significant.

## VI. CONCLUSION

In this paper, we have derived optimum and near-optimum receivers for differentially coherent reception in Adaptive Demodulation systems using 16-DPSK and 16-DAPSK. Simple decision rules were derived for the optimal demodulation of the  $\beta$  most likely bits for both 16-DPSK and 16-DAPSK. Although these simple rules led to simple decision schemes for 16-DPSK, the resulting decision schemes for 16-DAPSK contained nonlinear boundaries that were not conducive to a simple implementation. Based on the 16-DAPSK decision rules, heuristic near-optimal decision schemes were proposed for 16-DAPSK with a simple implementation; in addition, formulas were derived to tailor the decision schemes for any desired ring ratio. The probability of error for 16-DPSK and 16-DAPSK receivers demodulating the most reliable 1, 2, 3, and 4 bits per symbol was computed along with the spectral efficiency of the ADM systems.

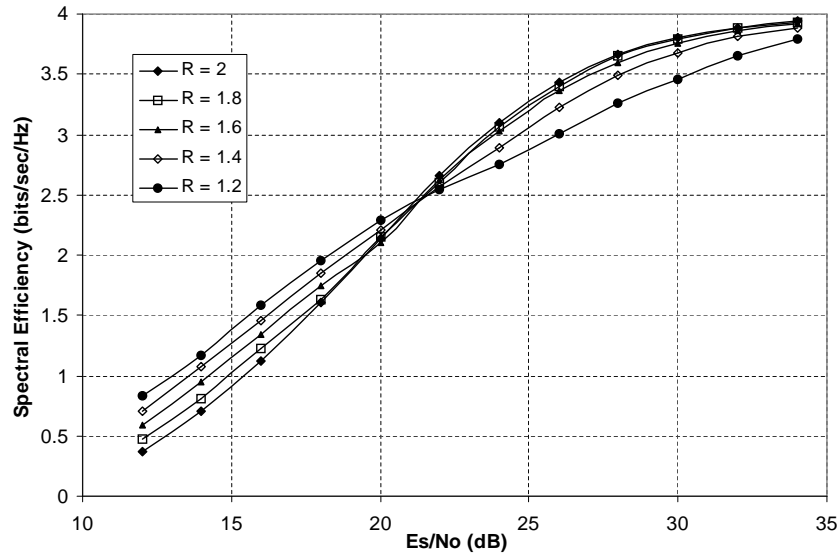


Fig. 11. Spectral Efficiency of 16-DAPSK for various ring ratios (raw BER of  $10^{-4}$ ).

A surprising result was demonstrated that over a large operating region, 16-DPSK actually outperforms 16-DAPSK for Adaptive Demodulation systems. The impact of the ring ratio on the spectral efficiency of ADM using 16-DAPSK was investigated and it was shown that ring ratios larger than 2 are never beneficial (in terms of spectral efficiency) for such systems. A tradeoff was shown to exist where low ring ratios improved the performance of 16-DAPSK for low average SNR operating regions, while larger ring ratios led to an improvement in the performance of high average SNR operating regions.

## REFERENCES

- [1] J. D. Brown, K. N. Plataniotis, and S. Pasupathy, "Adaptive demodulation with differentially coherent detection," in *Proc. of IEEE Int. Symposium on Personal, Indoor and Mobile Radio Communications (PIMRC'07)*, 2007.
- [2] J. S. Blogh and L. Hanzo, *Third-Generation Systems and Intelligent Wireless Networking: Smart Antennas and Adaptive Modulation*, John Wiley and Sons, 2002.
- [3] S. Nanda, K. Balachandran, and S. Kumar, "Adaptation techniques in wireless packet data services," *IEEE Communications Magazine*, vol. 38, no. 1, pp. 54–64, Jan. 2000.
- [4] P. Zhang and L. Li, "Research on beyond 3G mobile communications," in *Proc. of International Conference on Communications Technology*, April 2003, vol. 1, pp. 28–31.
- [5] A. J. Goldsmith and S.-G. Chua, "Variable-rate variable-power MQAM for fading channels," *IEEE Trans. on Commun.*, vol. 45, no. 10, pp. 1218–1230, Oct. 1997.

- [6] J. J. Metzner, "An improved broadcast retransmission protocol," *IEEE Trans. on Commun.*, vol. 32, no. 6, pp. 679–683, June 1984.
- [7] J. D. Brown, S. Pasupathy, and K. N. Plataniotis, "Adaptive demodulation using rateless erasure codes," *IEEE Trans. on Commun.*, vol. 54, no. 9, pp. 1574–1585, Sept. 2006.
- [8] J. D. Brown, *Adaptive Demodulation Using Rateless Erasure Codes*, Ph.D. Thesis, University of Toronto, 2008.
- [9] M. Luby, "LT codes," in *Proc. of the 43rd Annual IEEE Symposium on Foundations of Computer Science (FOCS)*, 2002, pp. 271–280.
- [10] A. Shokrollahi, "Raptor codes," *IEEE Trans. on Inform. Theory*, vol. 52, no. 6, pp. 2551–2567, June 2006.
- [11] X. Liu and T. J. Lim, "Fountain codes over fading relay channels," *IEEE Trans. on Wireless Commun.*, vol. 8, no. 6, pp. 3278–3287, June 2009.
- [12] K. Illanko and A. Anpalagan, "Cooperative communication using bit-selective adaptive demodulation and Raptor codes: The Gaussian relay channel case," in *Proc. of IEEE 69th Vehicular Technology Conference, VTC Spring, 2009*.
- [13] M. Stojanovic, "An adaptive algorithm for differentially coherent detection in the presence of intersymbol interference," *IEEE Journal on Selected Areas in Commun.*, vol. 23, no. 9, pp. 1884–1890, Sept. 2005.
- [14] J. S. Lee, R. H. French, and Y. K. Hong, "Error performance of differentially coherent detection of binary DPSK data transmission on the hard-limiting satellite channel," *IEEE Trans. on Inform. Theory*, vol. IT-27, no. 4, pp. 489–497, July 1981.
- [15] J. M. Kahn, "Modulation and detection techniques for optical communication systems," in *Proc. of Optical Amplifiers and Their Applications/Coherent Optical Technologies and Applications*. Technical Digest OAA/COTA06, paper CThC1, 2006.
- [16] J. G. Proakis, *Digital Communications*, New York: McGraw-Hill, forth edition, 2001.
- [17] J. Abouei, J. D. Brown, K. N. Plataniotis, and S. Pasupathy, "On the energy efficiency of LT codes in proactive wireless sensor networks," *Proc. of IEEE Biennial Symposium on Communication (QBSC'10), Kingston, Canada*, pp. 114–117, May 2010.
- [18] F. R. Kschischang, B. J. Frey, and H.-A. Loeliger, "Factor graphs and the sum-product algorithm," *IEEE Trans. on Inform. Theory*, vol. 47, no. 2, pp. 498–519, Feb. 2001.
- [19] W. C. Lindsey and M. K. Simon, *Telecommunication Systems Engineering*, Englewood Cliffs, NJ: Prentice-Hall, 1973.
- [20] L. Xiao, X. Dong, and T. T. Tjhung, "Maximum likelihood receivers for DAPSK signaling," *Journal of Communications and Networks*, vol. 8, no. 2, pp. 205–211, June 2006.
- [21] D. Divsalar and M. K. Simon, "Multiple-symbol differential detection of MPSK," *IEEE Trans. on Commun.*, vol. 38, no. 3, pp. 300–308, March 1990.
- [22] L. Xiao, *Signalling Constellations in Wireless Fading Channels*, M.Sc. Thesis, University of Alberta, 2004.
- [23] Y. C. Chow, A. R. Nix, and J. P. McGeehan, "Analysis of 16-APSK modulation in AWGN and Rayleigh fading channel," *Electron. Lett.*, vol. 28, pp. 1608–1610, Aug. 1992.
- [24] R. F. Pawula, S. O. Rice, and J. H. Roberts, "Distribution of the phase angle between two vectors perturbed by Gaussian noise," *IEEE Trans. on Commun.*, vol. 30, no. 8, pp. 1828–1841, Aug. 1982.
- [25] J. D. Brown, K. N. Plataniotis, and S. Pasupathy, "Adaptive demodulation performance over a Rayleigh fading channel," in *Proc. of 23rd Biennial Symposium on Communications*. Kingston, ON, Canada, May 2006, pp. 51–54.